ISSN: 0067-2904

Annealing effect on the structural and Morphological properties of Organic Semiconductor $Alq_3:C_{60}$ blend Thin Films

Husham N. Noori*, Lamiaa Kh. Abbas, Ameer F. Abdulameer
Department of Physics, College of Science, University of Baghdad, Baghdad, Iraq

Abstract

In this work, has been a studied the effect of thermal treatment using different annealing temperatures (373, 423 and 473) K in vacuum on structural and morphological properties of organic semiconductor $Alq_3:C_{60}$ thin films which are prepared by the spin coating on a glass, silicon and porous silicon. These films have been coated on substrates with speed of 2000 rpm. The structure properties of Tris(8-hydroxyquinoline) aluminum (III) (Alq_3) and fullerene (C_{60}) (100:1) and (100:10) blend as-deposited and treated have been studied by X-ray diffraction (XRD) for glass only and morphological properties by Atomic Force Microscope (AFM) for silicon and porous silicon substrates. The results of XRD pattern shows that the structure of ($Alq_3:C_{60}$) as-deposited and annealed thin films are polycrystalline in nature for both mixed weight ratio. The result of AFM measurements show that grain size increase is due to the increases of surface energy at high temperature. Surface roughness increasing and decreased randomly with the temperature can be attributed to the random distributions of the grains and also due to the phase change.

Keywords: Organic Semiconductors, $Alq_3:C_{60}$, Morphological Properties and heat treatment, porous silicon, roughness average, r.m.s roughness and average diameter

تأثير التلدين على الخصائص الطبوغرافية لاغشية مزيج أشباه الموصلات العضوية $Alq_3:C_{60}$ الرقيقة

هشام نصير*، لمياء خضير، أمير فيصل
قسم الفيزياء، كلية العلوم، جامعة بغداد، بغداد، العراق

الخلاصه

في هذا العمل تمت دراسة تأثير المعاملة الحرارية بأستخدام تلدينات حرارية مختلفة(373,423,473) كلفن بمعزل عن الهواء على الخصائص التركيبية والطبوغرافية لاغشية شبة الموصل العضوي $Alq_3:C_{60}$ المحضر بطريقة الطلاء البرمي على ارضية من الزجاج، سليكون والسليكون المسامي . تم طلاء تلك الاغشية على الارضية بسرعه دوران 2000 . تمت دراسة الخصائص التركيبية لمزيج المنيوم ثلاثي هيدروكسي كينولين (Alq_3) و الفولورين (C_{60}) كترسيب و معامل حرارياً بأستخدام حيود الاشعه السينية على الزجاج فقط و الخصائص الطبوغرافية بأستخدام مجهر القوة الذرية (AFM) للسليكون و السليكون المسامي. اوضحت نتائج نمط الاشعه ان تركيب ($Alq_3:C_{60}$) كترسيب و معامل حرارياً ذو طبيعه متعدده التبلور لكلا النسبتين الممزوجتين. أوضحت نتائج قياسات AFM زياده الحجم الحبيبي نتيجة لزيادة الطاقة السطحية عند درجات الحراره العالية . يعزى تتزايد وتتناقص خشونة السطح بصورة عشوائية مع درجة الحرارة الى التوزيع العشوائي للحبيبات وايضاً نتيجة لتغير في الطور .

*Email: Husham _Naseer@yahoo.com

Introduction

Organic semiconductors are organic materials with semiconductor properties, which consist in general of carbon atoms (C) [1]. The interest in organic semiconductors for use in organic lighting emitting diodes (OLEDS) started with the report [2] of efficient green electroluminescence from Tris-(8-hydroxyquinoline) aluminum (Alq_3). The chemistry of the fullerene C_{60} particle has been the topic of very concentrated study always since the large scale fabrication of this composite was reported [3]. Despite of synthesized and studied of organic semiconducting but the performance and stability of this materials were poor [4]. The performance of the organic materials can be increased by making improvement in the fabrication of the device rather than focusing on the complexity of the internal structure of the material [5]. Small molecules and polymer are types of organic semiconductors according to the molecular size [6]. Tris-(8-hydroxyquinoline) aluminum (Alq_3) is π-conjugated small molecule (low-molecular weight) [7], and one of the most important materials between the class of organometallic compounds, which used as active medium in organic light emitting Diodes (OLEDs) [8], as show in fig 1a. Fullerenes C_{60} are represent the third allotrope form of pure carbon, after graphite and diamond and have acquired interest in many fields of science that range from bio applications to molecular electronics [9]. In this research, the structural and morphological properties of the blend Alq_3:C_{60} thin films were studied with different concentrations of C_{60}, as show in Figure-1(b).

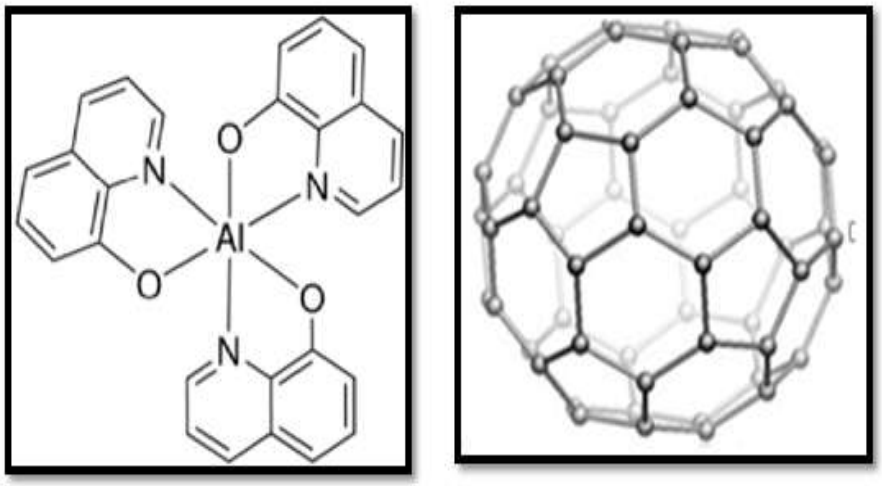

Figure1- Chemical structure of: a. Tris-(8-hydroxyquinoline) aluminum (Alq_3) and b. fullerene C_{60} [10, 11].

2. Experimental work

Tris-(8-hydroxyquinoline) aluminum (Alq_3) and Fullerenes C_{60} were purchased from sigma-Aldrich and used without further purification. The molecular formula of Tris-(8-hydroxyquinoline) aluminum (Alq_3) is $Al(C_9H_6NO)_3$ and has 459.441g/mol, while Fullerenes (C_{60}) is 720.66 g/mol. Before deposition the blend, the glass substrate cut to the size of 2.5cm×2.5cm after that cleaned in an ultrasonic bath for 10 min, to remove the dirt particles on the substrate surface using different steps with distilled water, liquid soap, a solution of ethanol and acetone. The first blend prepared by dissolving 15 g/ml for alq3 in chloroform with 100:1 weigh ratio and 0.15 g/ml C60 in toluene while the second blend prepared by dissolving 15 g/ml for alq_3 in chloroform and 1.5 g/ml C_{60} in toluene with 100:10 weigh ratio. This solution putted on a magnetic stirrer for 24 hour at 45C. Then they filtered using 0.2 and 0.45 micrometer respectively. Finally the two solutions of alq_3 and C_{60} were blended together and putted on the stirrer again for 24 hour also to get homogenous solution. A mono crystalline silicon wafers p- type, doped with boron with resistivity range (Ω =0.01-0.02Ω.cm), orientation (100) and thickness (525 µm). Porous silicon was prepared by electrochemical etching with condition current 12 mA and 15 min. Now the blended solution becomes ready to spin-coated method type CHEMAT SCIETIFIC SKW-4A2 on the pre-cleaned glass, silicon and porous silicon substrate for 2000 rpm. The prepared samples with thickness 100nm, was left in air for one day then putted in an oven at 70^{o}C for 15min to remove the residual solvent may be stay inside the film as (tiny) Nano bubbles. The prepared (Alq3: C_{60}) thin films was annealed in a vacuum oven at different temperatures (373, 423 and 473) K for almost one hour. The pattern of X-Ray Diffraction has been plotted the

intensity as a function of Braggs angle. This analysis was using x-ray diffracometric system type Shimadzu XRD 6000. While the morphology of blends study by Atomic Force Microscope (AFM) in college of science chemistry.

3. Results and Discussions

The structural characterization bulk heterojunction BHJ blend (Alq_3:C_{60}) thin film spin coated at room temperature and heat treated films at temperatures (373, 423, 473) K were recorded by X-ray diffraction in the range of 2θ between 0 to 50^o as shown in Figures-(2, 3).

In first weigh ratio (100:1), it is found that there are 11 diffraction peaks at different Bragg angles, 2θ^o= 6.320, 7.285, 7.85, 10.111, 11.276, 12.772, 13.696, 14.634, 15.698, 16.622, and 17.882 degree corresponding to reflection surfaces hkl {(101), (010), (1$\bar{1}$0), (001), (011), (101), (100), (101), (111) and (220)} respectively, and this is and this result is in good agreement with Cölle and Brütting[12,13]. XRD analysis indicate that the structure of Alq_3 is polycrystalline in nature with characteristic planes of α phase. Also, the films are crystallized with a strong peak at (1$\bar{1}$0) direction in BHJ structure, this means that this plane is suitable for crystal growth [14]. The increase of the plane intensity could be attributed to the increase in crystalline (grin) size as the small crystals coalescence each other when films annealing at room temperature [14]. While this peak disappeared gradually in XRD pattern of annealed films with Ta=423K and Ta=473K and this may be due to the change of crystallites orientation and vibration of atom in plane.

It was observed that the well-defined peaks (220) and (111) at RT and 473K respectively in this pattern, correspond to the relative increase in ordered crystalline structures. In this pattern those peaks are thin (small) sand correspond to main phase of the C_{60} fullerene molecule ordered in a face-centered cubic structure of higher symmetry which is included in the BHJ blend of Alq_3:C_{60} thin films. In this model a broad peak, in the range between 15 and 26 degrees can be observed, this peak is crowned by other well defined low intensity peaks, corresponding to lower symmetry phases C_{60} ordered in orthorhombic and monoclinic structures [15].

For second weigh ratio (100:10), it is found that there are 7 diffraction peaks at different Bragg angles, 2θ= 6.299, 7.216, 7.851, 11.365, 15.760, 16.806, and 17.795 degree corresponding to reflection surfaces (101), (010), (1$\bar{1}$0), (011), (101), (101) and (220) respectively, and this is in relatively agreement with Cölle and Brütting . These peaks corresponding to Alq_3 with phase α. For C_{60} the well-defined peak (220) in these patterns corresponds to the highly ordered crystalline structures and the peak (111) disappears in second ratio. The disappearing of some peak corresponding to Alq_3 and C_{60} in thin films of the ratio (100:10) may be due to the increasing in amorphosity in these films caused by adding more quantity from C_{60}, or may be due to the amorphous nature with some crystalline peak in the XRD patterns for both Alq_3 and C_{60} thin films corresponds to a large distribution of possible molecular packing's when the powder has been diluted in solvent and spin-coated onto glass substrates [16-18].

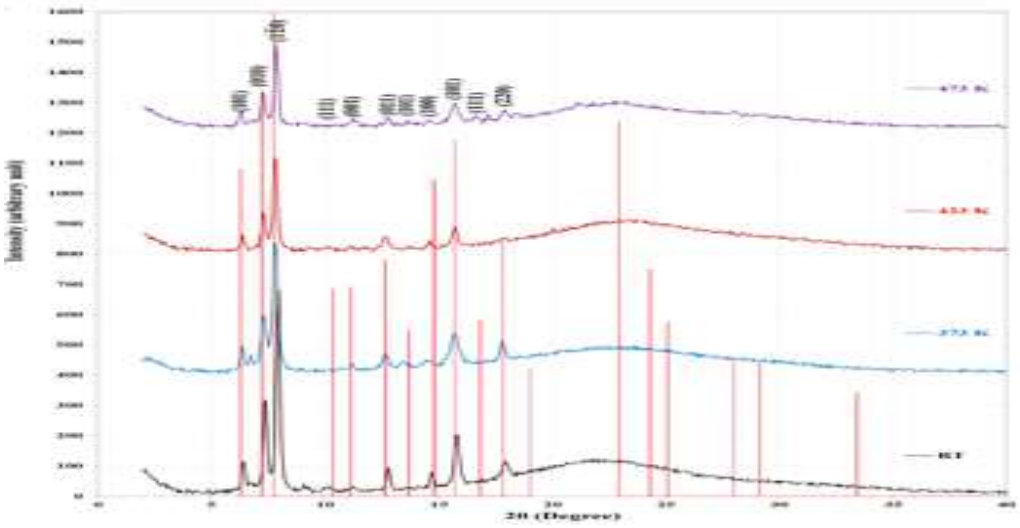

Figure 2:-XRD pattern of as-deposited and annealing temperature blend (Alq_3/ C_{60}) thin films. (100:1).

Table 1-The structural parameters of as-deposited and annealed (Alq_3:C_{60})(100/1)wt%thin Films Thin Films

T_a(K)	2θ (Deg)	FWHM (Deg)	d_{hkl} Exp.(Å)	G.S (nm)	hkl	Phase
RT	6.4223	0.1856	13.7515	42.9	(101)	Alq_3
	7.3767	0.1822	11.9744	43.7	(010)	Alq_3
	7.9476	0.1834	11.1154	43.4	(1$\bar{1}$0)	Alq_3
	10.1113	0.3702	8.7412	21.6	(111)	Alq_3 C60
	11.2262	0.2487	7.8754	32.1	(001)	Alq_3
	12.7969	0.1834	6.9121	43.6	(011)	Alq_3
	14.7117	0.1845	6.0165	43.4	(020)	Alq_3
	15.8167	0.2442	5.5986	32.9	(101)	Alq_3
	17.9452	0.3105	4.9390	25.9	(220)	Alq_3 C60
373	6.3623	0.1859	13.8811	42.8	(101)	Alq_3
	7.3017	0.2473	12.0972	32.2	(010)	Alq_3
	7.8210	0.2471	11.2950	32.2	(1$\bar{1}$0)	Alq_3
	11.1846	0.1854	7.9046	43.1	(001)	Alq3
	12.6715	0.3094	6.9802	25.8	(011)	Alq_3
	14.5269	0.3717	6.0926	21.6	(100)	Alq_3
	15.7120	0.4329	5.6356	18.5	(101)	Alq_3
	17.8145	0.2475	4.9750	32.5	(220)	Alq_3 C60
423	6.3801	0.1859	13.8423	42.8	(101)	Alq_3
	7.2955	0.1859	12.1074	42.8	(010)	Alq_3
	7.8217	0.1859	11.2940	42.8	(1$\bar{1}$0)	Alq_3
	11.0875	0.1857	7.9736	43.0	(001)	Alq_3
	12.6932	0.3095	6.9683	25.8	(011)	Alq_3
	14.6128	0.1238	6.0570	64.7	(100)	Alq_3
	15.7177	0.2476	5.6336	32.4	(101)	Alq_3
473	6.3201	0.1847	13.9735	43.1	(101)	Alq_3
	7.2853	0.1854	12.1244	43.0	(010)	Alq_3
	7.8565	0.1833	11.2441	43.5	(1$\bar{1}$0)	Alq_3
	11.2760	0.3108	7.8408	25.7	(001)	Alq_3
	12.7723	0.2488	6.9254	32.1	(011)	Alq_3
	13.6965	0.2488	6.4601	32.2	(101)	Alq_3
	14.6345	0.1868	6.0481	42.9	(100)	Alq_3
	15.6987	0.2476	5.6404	32.4	(101)	Alq_3
	16.6228	0.3116	5.3288	25.8	(111)	Alq_3
	17.8821	0.2489	4.9563	32.3	(220)	Alq3 C60

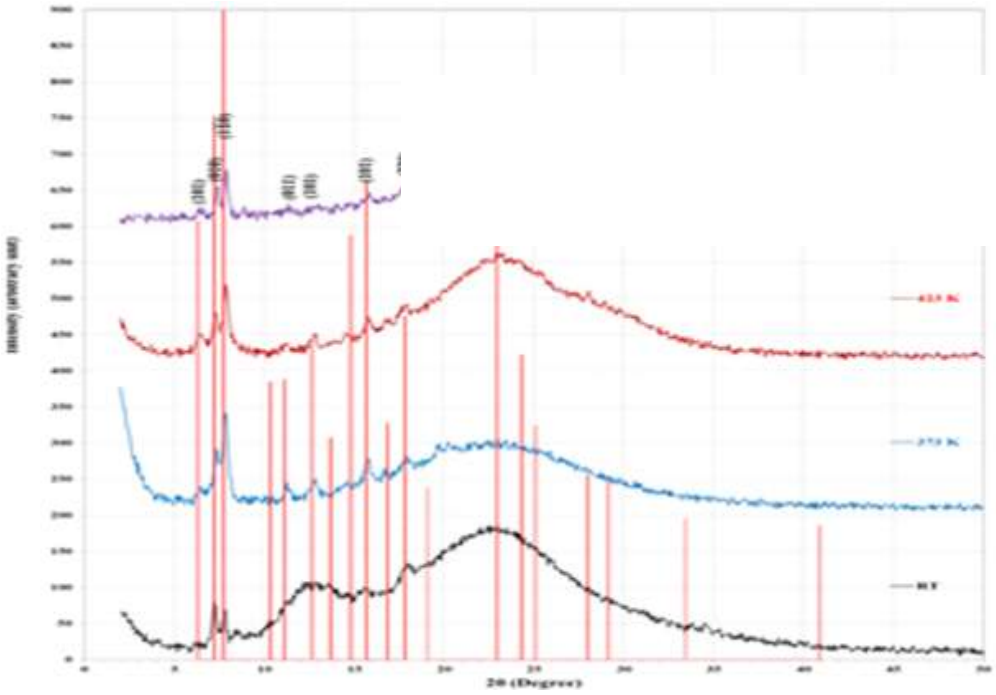

Figure 3-XRD pattern of as-deposited and annealing temperature blend (Alq_3/ C_{60}) thin films. (100:10).

Table 2-The structural parameters of as-deposited and annealed (Alq_3:C_{60})(100/10)wt% thin Films Thin Films

T_a(K)	2θ (Deg.)	FWHM (Deg.)	d_{hkl} Exp.(Å)	G.S (nm)	hkl	phase
RT	6.2991	0.3467	14.0201	23.0	(101)	Alq3
	7.2162	0.2594	12.2403	30.7	(010)	Alq3
	7.7511	0.2594	11.3967	30.7	(1$\bar{1}$0)	Alq3
	11.1135	0.3107	7.9550	25.7	(011)	Alq3
	15.7607	0.3738	5.6183	21.5	(101)	Alq3
	16.8066	0.4973	5.2710	16.2	(101)	Alq3
	17.7956	0.6224	4.9802	12.9	(101)	Alq3:C60
373	6.2991	0.3467	14.0201	23.0	(101)	Alq3
	7.2162	0.2594	12.2403	30.7	(010)	Alq3
	7.7511	0.2594	11.3967	30.7	(1$\bar{1}$0)	Alq3
	11.2430	0.3107	7.8637	25.7	(011)	Alq3
	12.7925	0.3098	6.9145	25.8	(101)	Alq3
	15.7607	0.3738	5.6183	21.5	(101)	Alq3
	16.8066	0.4973	5.2710	16.2	(101)	Alq3
	17.7956	0.6224	4.9802	12.9	(220)	Alq3:C60
423	6.2991	0.3467	14.0201	23.0	(101)	Alq3
	7.2162	0.2594	12.2403	30.7	(010)	Alq3
	7.7511	0.2594	11.3967	30.7	(1$\bar{1}$0)	Alq3
	11.2077	0.3114	7.8884	25.6	(011)	Alq3
	12.7621	0.3119	6.9309	25.6	(101)	Alq3
	15.7607	0.3738	5.6183	21.5	(101)	Alq3
	16.8066	0.4973	5.2710	16.2	(101)	Alq3
	17.7956	0.6224	4.9802	12.9	(220)	Alq3:C60
473	6.2991	0.3467	14.0201	23.0	(101)	Alq3
	7.2162	0.2594	12.2403	30.7	(010)	Alq3
	7.7511	0.2594	11.3967	30.7	(1$\bar{1}$0)	Alq3
	11.3652	0.3090	7.7794	25.8	(011)	Alq3
	15.7607	0.3738	5.6183	21.5	(101)	Alq3
	16.8066	0.4973	5.2710	16.2	(101)	Alq3
	17.7956	0.6224	4.9802	12.9	(220)	Alq3:C60

The primary purpose of the use of an atomic force microscope (AFM) was to study the surface nanostructure of the BHJ Alq_3:C_{60} thin film. AFM system is useful technique, capable of drawing three and two-dimensional images of the surface of the Alq_3:C_{60} organic thin films and clarify the morphological changes in organic thin films at different thermal annealing temperatures. Figures- (4 to 7) shows AFM micrographs {roughness average, r.m.s roughness, average diameter (grain size), and peak to peak} of the Alq_3:C_{60} thin films deposited by spin coated on Si and PS-Si with two concentration weight ratio (100:1) and (100:10) at room temperature and various thermal annealing temperatures (373, 423 and 473) K.

The average roughness (R_a) can be used to describe the sharpness of the films' surface. That is, the average roughness is defined as the mean height of the surface from the center of the plane in a given area [19]. Root mean square (r.m.s) roughness defined as the standard deviation of the surface height profile from the average height, is the most commonly reported measurement of surface roughness [20].

The surface microstructure of (100:1) Alq_3: C_{60} / Si, (100:10) Alq_3: C_{60} / Si, (100:1) Alq_3: C_{60} / Ps, (100:10) Alq3: C60 / Ps thin films were carried out by AFM. Fig. 4 to 7 indicates the 3D& 2D AFM images (100:1) Alq_3: C_{60} / Si, (100:10) Alq_3: C_{60} / Si, (100:1) Alq_3: C_{60} / Ps, (100:10) Alq_3: C_{60} / Ps thin films at different annealing temperature varied at RT, 373K, 423K and 473K.

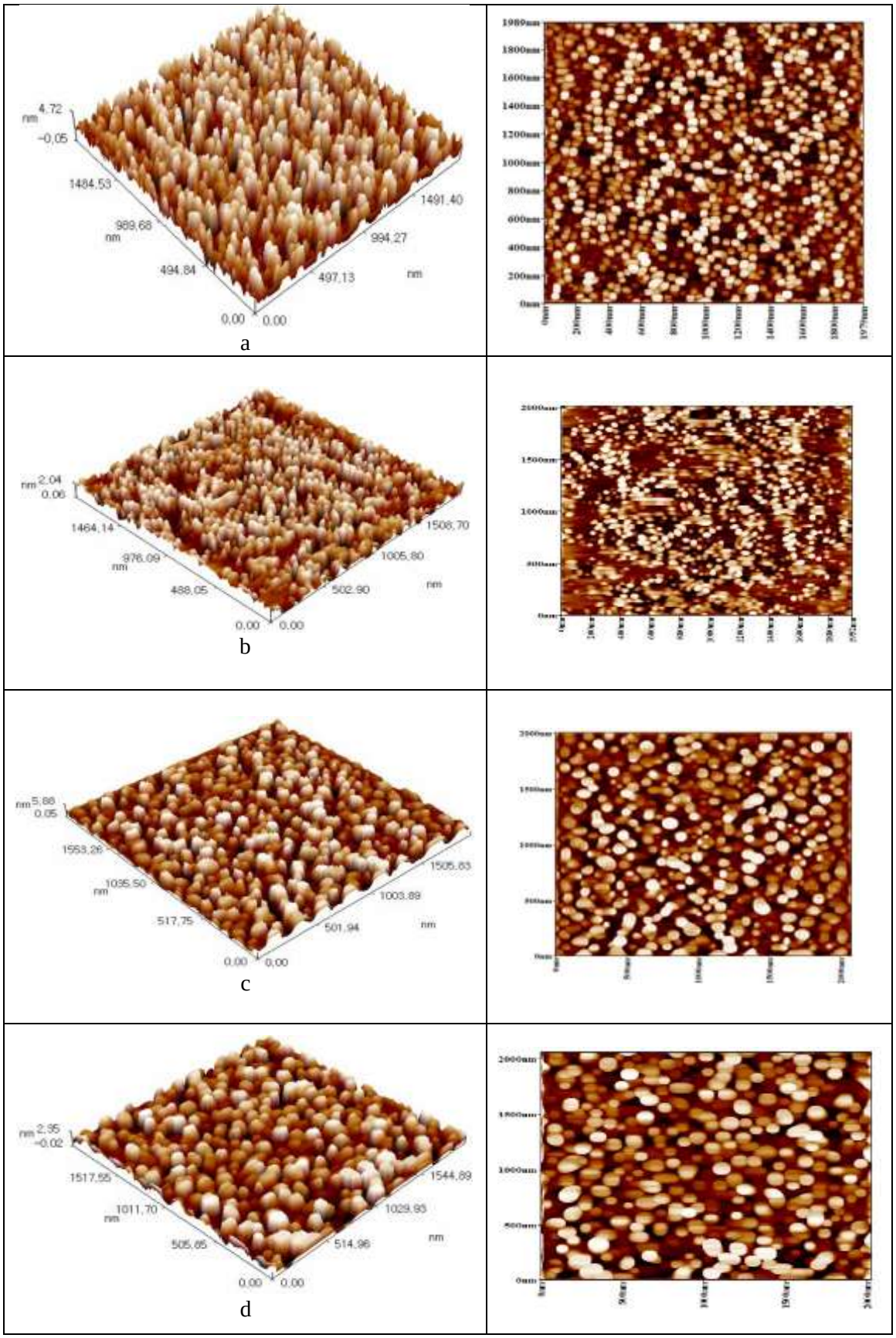

Figure 4-3D& 2D AFM images of (100:1) Alq3: C60 / Si thin film at (a) as-deposited (b) Ta=373 K (c) Ta=423K (d) Ta=473K

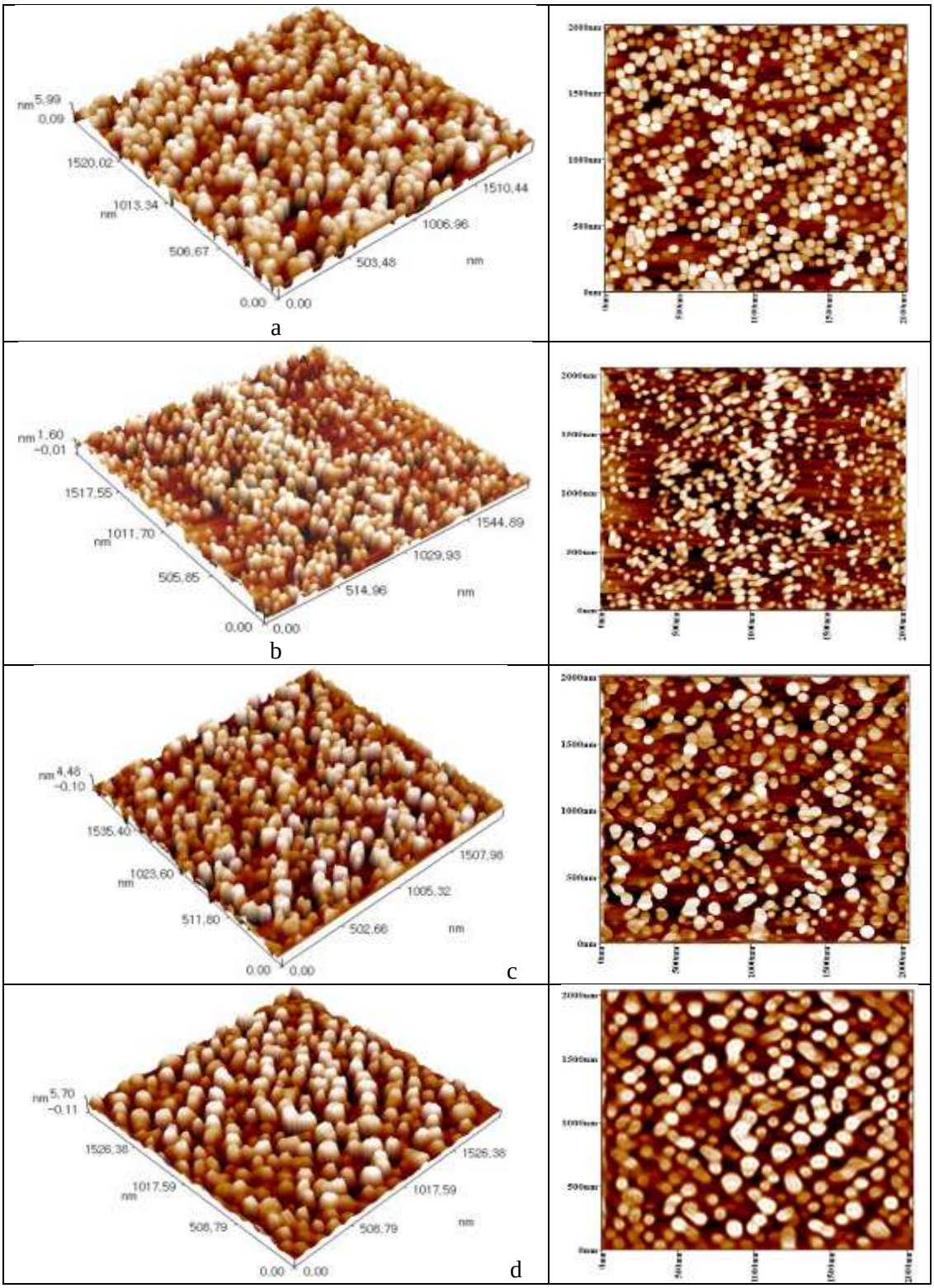

Figure 5-3D& 2D AFM images of (100:10) Alq3: C60 / Si thin film at (a) as-deposited (b) Ta=373 K (c) Ta=423K (d) Ta=473K

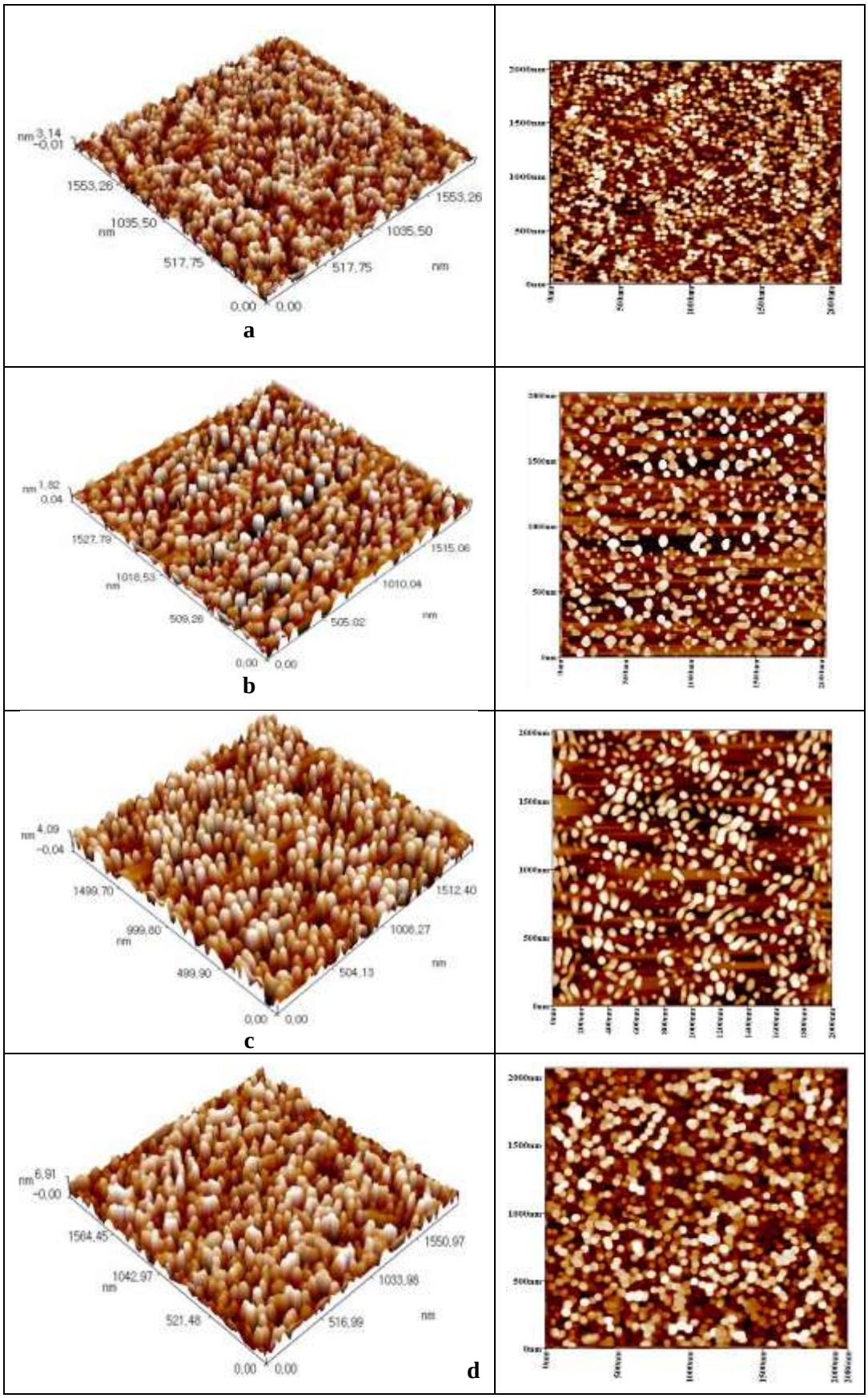

Figure 6-3D& 2D AFM images of (100:1) Alq3: C60 / PS thin film at (a) as-deposited Ta=373 K (c) Ta=423K (d) Ta=473K

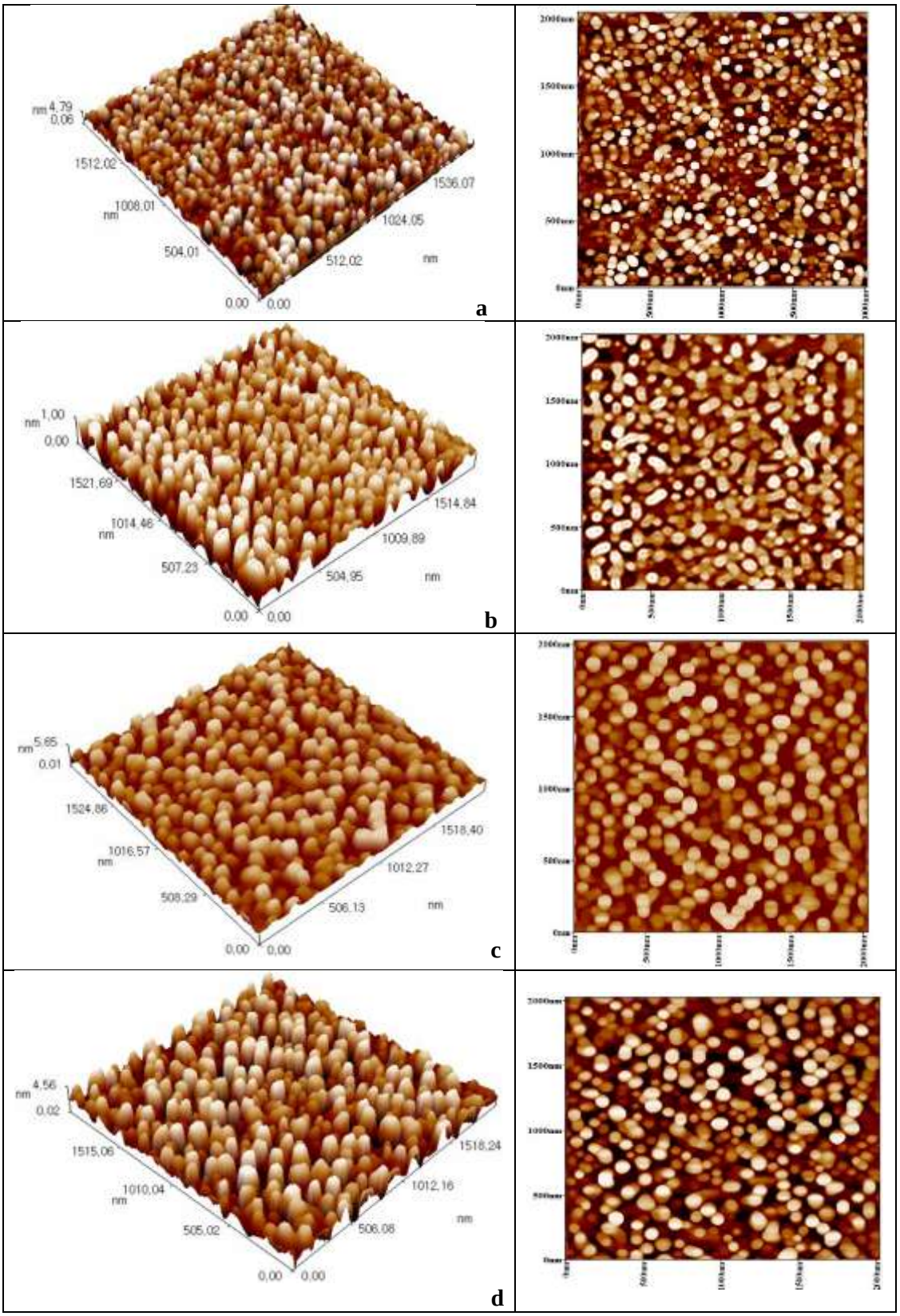

Figure 7-3D& 2D AFM images of (100:10) Alq3: C60 / PS thin film at (a) as-de posited (Ta=373 K (c) Ta=423K (d) Ta=473K

Table 3-Grain size, Roughness average and peak to peak (nm) of deposited and annealed Alq_3: C_{60}/ Si and Alq3: C60 / PS thin films.

(100:1) Alq3: C60 / Si				
T_a K	**Roughness Average (nm)**	**r.m.s roughness**	**Avg. Diameter (grain size) (nm)**	**Peak to peak (nm)**
RT	1.19	1.38	46.54	4.67
373	0.496	0.572	57.76	1.98
423	1.4	1.64	64.76	5.83
473	0.588	0.681	85.13	2.37
(100:10) Alq3: C60 / Si				
T_a K	**Roughness average (nm)**	**r.m.s roughness**	**Avg. Diameter (grain size) (nm)**	**Peak to peak (nm)**
RT	1.40	1.64	49.78	5.9
373	0.403	0.465	62.09	1.61
423	1.14	1.32	66.33	4.75
473	1.42	1.66	89.94	5.81
(100:1) Alq3: C60 / PS				
T_a K	**Roughness average (nm)**	**r.m.s roughness**	**Avg. Diameter (grain size) (nm)**	**Peak to peak (nm)**
RT	0.792	0.913	35.00	3.15
373	0.466	0.515	47.45	1.78
423	1.03	1.19	63.50	4.13
473	1.63	1.89	77.93	6.91
(100:10) Alq3: C60 / PS				
T_a K	**Roughness average (nm)**	**r.m.s roughness**	**Avg. Diameter (grain size) (nm)**	**Peak to peak (nm)**
RT	1.18	1.36	41.61	4.73
373	0.219	0.26	50.94	1
423	0.893	1.02	70.74	4.74
473	1.13	1.31	79.68	4.44

The root mean square (RMS) surface roughness, obtained from AFM images corresponding to (100:1) Alq_3: C_{60} / Si, (100:10) Alq_3: C_{60} / Si, (100:1) Alq_3: C_{60} / Ps, (100:10) Alq_3: C_{60} / Ps thin films, is listed in Table 3. . Based on the results obtained, the grain and grain boundaries are not obviously seen. However, there is particles overlap which beliefs to be stacking grains. The AFM results show that the size of the grains increased as the annealing temperature increased to 473K. This increasing in grain size is due to the increases of surface energy at high temperature. The grain growth mechanism happens due to the transfer of atoms at higher temperature have sufficient diffusion activation energy to occupy the crystal lattice and induced the small grains by grain boundary diffusion thus the grains form in larger size [21].

The obtained results of surface roughness at RT annealing temperature from table 1 for all films have certain value then with the increasing of temperature the surface roughness (SR) decreased then when continuously increasing the temperature the SR for the films increased also at 473K annealing temperature. This behavior can be attributed to the random distributions of the grains and also due to the phase change. It can be concluded that low roughness of all films was at high 473K annealing

temperature. Or this different in morphology of the surfaces for annealed and un-annealed Alq_3: C_{60} / PS and Alq_3: C_{60} / PS is may be induced by presence of C_{60} in structure of this blend.

4. Conclusion

- The XRD pattern showed that the structure of (Alq_3:C_{60}) as-deposited and annealed BHJ thin films are polycrystalline in nature for both mixed weight ratio.
- Crystallite size increase is due to the increases of surface energy at high temperature. Surface roughness increasing and decreased randomly with the temperature can be attributed to the random distributions of the grains and also due to the phase change.

Reference

1. Christof Wöll. **2009.** *Organic Electronics Structural and Electronic Properties of OFETs*. WILEY-VCH Verlag GmbH & Co. KGaA, Weinheim.
2. Tang, C.W. and Van Slyke, S.A. **1987.** Organic electroluminescent diodes. *Appl. Phys. Lett*. **51**: 913.
3. Kratschmer, W., Lamb, L.D., Fostiropoulous, and D. R. Huffman, D. R. **1990.** Solid C_{60}: a new form of carbon**.** *Nature*, : 347-354.
4. Gutmann, F. and Lyons, L.E. **1967.** *Organic Semiconductors*. John Wiley & Sons.
5. Kowalsky, W., Becker, E., Benstem, T., Dobbertin, T., Johannes, H., Metzdorf, D., Neuner, H. and Sch¨obel, J. **2000.** Organic semiconductors fundamentals and applications, *Annual report*.
6. Marco Stella. **2009.** Study of Organic Semiconductors for Device Applications. Universtat De Barcelona, Doctor Barcelona, December.
7. Wanfeng Xie, Zhiyong Pang , Yu Zhao , Feng Jiang , Huimin Yuan, Hui Song Shenghao Han.**2014**. Structural and optical properties of ε-phase Tris (8-hydroxyquinoline) aluminum crystals prepared by using physical vapor deposition method. *Journal of Crystal Growth*, **404** (2014): 164–167.
8. Zawadzka, Płóciennik J., Strzelecki, Z. and Łukasiak, B. Sahraoui. **2014.** Photophysical properties of Alq_3 thin films. *Optical Materials*, **36**: 91–97.
9. Maya Shankar Singh. **2004.** *Advanced Organic chemistry: Reactions and Mechanisms*. Pearson Education India.
10. Curioni, and W. Andreoni, **1998.** Atom-resolved electronic spectra for Alq_3 from theory and experiment**.** *Applied physics letters*, **72**: 1575-1577, 13.
11. Konarev, D. V. and R N Lyubovskaya. R.N. **1999**. Donor - acceptor complexes and radical ionic salts based on fullerenes. *Russian Chemical Reviews*, **68**(1): 19 - 38.
12. Myers. H. p. **2002.** *Introductory Solid State Physics*. Taylor & Francis. ISBN 0-7484-0660-3.
13. Curry, R.J., Gillin, W.P., Clarkson, J. and Batchelder. D.N. **2002.** Morphological study of aluminum Tris (8-hydroxyquinoline) thin films using infrared and Raman spectroscopy. *Journal of applied physics*, **92**: 1902-1905, 4.
14. Cölle, M. and Brütting, W. **2004.** Thermal, structural and photophysical properties of the organic semiconductor Alq_3**.** *Phys. Stat. Sol*. (a) 201. 1095, (6).
15. Hussein, M.M.A., Abdullah, M.M. and Mohammed, G.H. **2013.** Effect of Annealing and Deposition Temperature on Structural Properties of CdTe Thin Films Prepared by Thermal Evaporation Method**.** *Indian Journal of Applied Research*, **3**(2).
16. Jacobo Martínez-Reyes et.al, Lucia Graciela Díaz Barriga-Arceo, Luis Rendón-Vazquez, Reynaldo Martínez-Guerrero, Néstor Romero-Partida, Eduardo Palacios-González, Vicente Garibay-Febles, Jaime Ortiz-López. **2012.** Microstructural Characterization of Large Area C_{60} Films Obtained by Conventional Microwave Oven Irradiation. *World Journal of Nano Science and Engineering*. **2**: 213-218.
17. DJurisic, A.B., Lau, T.W., Kwong, C.Y., Lam, L.S.M., W. K. Chan, W.K. **2003**. Evaluation of optical tris (8-hydroxyquinoline) aluminium (Alq_3) with atmosphere exposure. *Proc. Of spie*, **4800**. Organic Light Emitting Materials and Device.
18. Cuba, M. and Muralidharan, G. **2014**. *Effect of thermal annealing on the structural and optical properties of tris-(8-hydroxyquinoline) aluminum (III) (Alq3) films*. John Wiley & Sons, Ltd. http://dx.doi.org/10.1002/bio.2738

19. Guan-Ting Chen, Shui-Hsiang Su, Cheng-Chieh Hou, and Meiso Yokoyama**. 2007.** "Effects of Thermal Annealing on Performance of Organic Light-Emitting Diodes"**,** Journal of The Electrochemical Society, 154 (5) J159-J162.
20. Ho Soonmin, "Atomic Force Microscopy Studies on the Surface Morphologies of Chemical Bath Deposited Cus Thin Films"**.** INTI International University, Putra Nilai, 71800, Negeri Sembilan, MALAYSIA.
21. Raship, N.A., Sahdan, M.Z., Adriyanto, F., M. F. Nurfazliana, M.F. and Bakri**,** A.S. **1788**. "Effect of annealing temperature on the properties of copper oxide films prepared by dip coating technique", AIP Conference Proceedings 1788, 030121.